Since January 2020 Elsevier has created a COVID-19 resource centre with free information in English and Mandarin on the novel coronavirus COVID-19. The COVID-19 resource centre is hosted on Elsevier Connect, the company's public news and information website.

Bioorganic Chemistry 116 (2021) 105309

Contents lists available at ScienceDirect

Bioorganic Chemistry

journal homepage: www.elsevier.com/locate/bioorg

Polyketone metabolites isolated from *Rhodiola tibetica* endohytic fungus *Alternaria* sp. HJT-Y7 and their SARS-CoV-2 virus inhibitory activitives

Xuan Lu [a,*], Xiao-Yuan Tang [a], Hai-Xin Wang [a], Wei-jin Huang [b], Wei-Xing Feng [a], Bao-Min Feng [a]

[a] College of Life Science and Biotechnology, Dalian University, Dalian 116622, China
[b] AIDS Department, Institute of Biological Products, China Food and Drug Testing Institute, Beijing 102629, China

ARTICLE INFO

Keywords:
Alternaria sp.
Rhodiola tibetica
Polyketone
SARS-CoV-2 virus

ABSTRACT

Six new polyketone metabolites, compounds (**1**–**6**) and seven known polyketone compounds (**7**–**13**) were isolated from *Rhodiola tibetica* endophytic fungus *Alternaria* sp. The structural elucidation of five new polyketone metabolites were elucidated on the basis of spectroscopic including 2D NMR and HRMS and spectrometric analysis. Inhibition rate evaluation revealed that compounds **1**(EC_{50} = 0.02 mM), **3**(EC_{50} = 0.3 mM), **6**(EC_{50} = 0.07 mM), **8**(EC_{50} = 0.1 mM) and **9**(EC_{50} = 0.04 mM) had inhibitory effect on the SARS-CoV-2 virus.

1. Introduction

Rhodiola tibetica is a plant of Rhodiola L., a perennial herbaceous plant unique to China, distributed in the Tibetan Plateau of Tibet Autonomous Region.[1] Rhodiola tibetica is recorded in the Tibetan medicine book more than 1,200 years in "Tibetan Medicine History". Plant endophyte is a microorganism including bacteria, actinomycete and fungi, which spends the whole or part of its life cycle colonizing inter- and/or intra-cellularly inside the healthy tissues of the host plant, typically causing no apparent symptoms of disease.[2] As an important part of the plant microecosystem, the special living environment of this type of microorganism determines the structure and activity diversity of its secondary metabolites. Therefore, plant endophytes are an important source of new structural compounds with biological activity.[3] This paper reported the isolation and structural elucidation of six new polyketone metabolites (**1**–**6**) and seven known polyketone compounds (**7**–**13**) from the *Rhodiola tibetica* endophytic fungus *Alternaria* sp. HJT-Y7. The inhibition tests and cytotoxicity tests of the Compounds **1**–**11** and **13** against SARS-CoV-2 virus were evaluated. The average EC_{50} (50% effctive concentration) and CC_{50} (50% cytotoxic concentration) values were recorded. On the basis of the comparison with control group on the SI index (SI = CC_{50}/average EC_{50}), the results showed that compounds **1**, **3**, **6**, **8** and **9** had inhibitory effect on the virus. Furthermore, **6** and **8** showed the significant inhibitory effect. These 5 compounds had potential druggability.

2. Results and discussion

2.1. Separation and identification of compounds

The fermentation product of *Alternaria* sp. HJT-Y7 were extracted with methanol. Column chromatography and preparative high-performance liquid chromatography (HPLC) were used for the separation and further purification of six new polyketone metabolites (**1**–**6**) and seven known polyketone compounds (**7**–**13**) (Fig. 1).

Alternaria A (**1**) was obtained as light yellow powder (MeOH), $[\alpha]_D^{20}$ —20 (*c* 0.2, MeOH). The molecular formulas of **1** was $C_{35}H_{36}O_9$ on the basis of highresolution electrospray ionisation mass spectrometry (HRESIMS) data $[M + Na]^+$ ion peak at *m/z* 623.2248 and was confirmed by the ^{13}C NMR, ^1H NMR spectroscopic (Table 1). The ^{13}C NMR and HMQC of **1** showed thirteen sp^2 quaternary carbons (δ_C 103.0, 104.7, 125.0, 126.5, 127.9, 131.2, 134.3, 136.7, 141.1, 151.9, 154.0, 155.9, 173.0), twelve sp^2 methine carbons (δ_C 113.6, 114.7, 115.0, 120.2, 122.0, 127.1, 127.5, 128.5, 129.0, 131.1, 131.2, 131.2), four sp^3 methylene carbons (δ_C 28.0, 34.7, 56.6, 57.0), two methyl groups (δ_C 15.9, 16.4), one oxymethyl carbon (δ_C 51.7). The 1H NMR spectrum of **1** showed signals attributable to three vicinal sp^2 spin networks [δ 6.79 (1H, d, J = 8.0 Hz), 6.85(1H, d, J = 8.0 Hz), 7.11(1H, t, J = 8.0 Hz)], [δ 6.46 (1H, d, J = 8.5 Hz), 6.61(1H, d, J = 8.5 Hz)], [δ 6.63 (1H, d, J = 8.0 Hz), 6.74(1H, d, J = 8.0 Hz), 7.00(1H, t, J = 8.0 Hz)]. The heteronuclear multiple bond correlation (HMBC) experiments (Fig. 2) showed the three aromatic moieties of **1** and the connectivity between group and carbons. The whole structure was divided into three fragments (Fig. 3)

* Corresponding author.
E-mail address: luxuan@dlu.edu.cn (X. Lu).

https://doi.org/10.1016/j.bioorg.2021.105309
Received 18 June 2021; Received in revised form 20 August 2021; Accepted 25 August 2021
Available online 28 August 2021

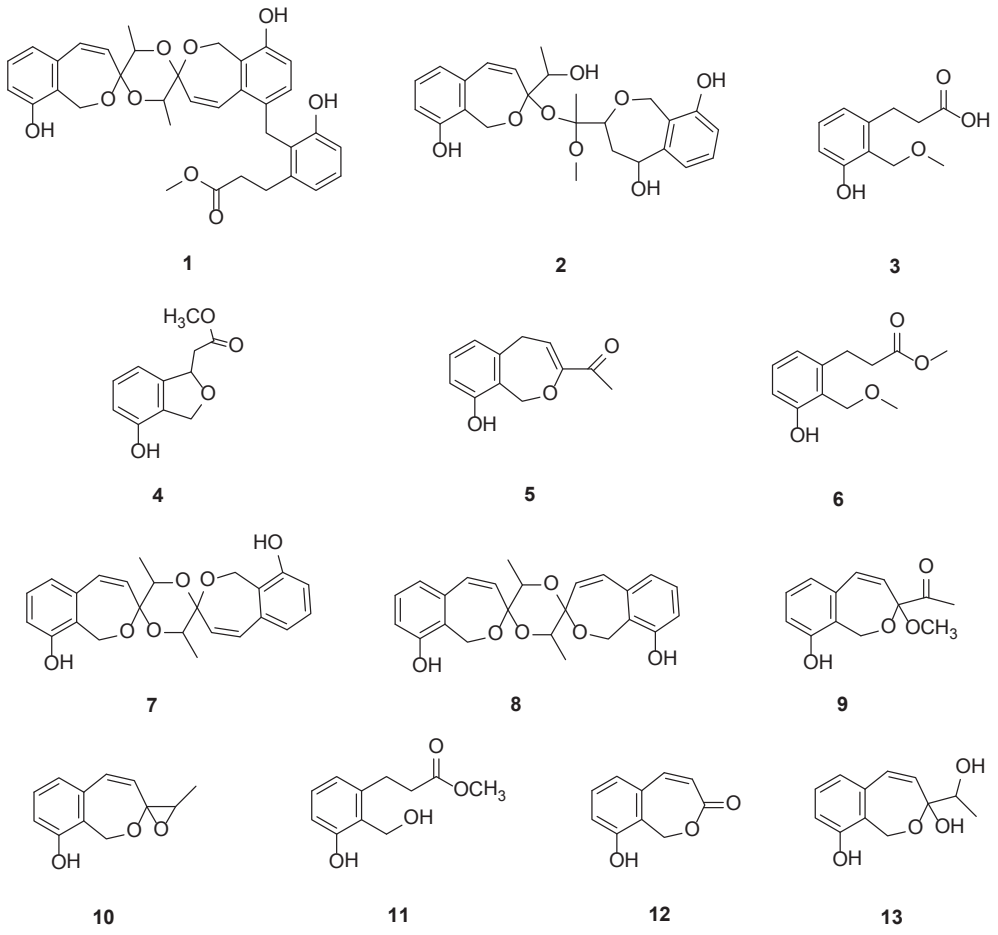

Fig. 1. Structures of compounds **1**–**13** from *Alternaria* sp. HJT-Y7.

according to the aromatic moieties, and each aromatic moiety possessed a phenolic OH. HMBC correlations about fragment **1-a** from H-4 [6.79 (1H, d, $J = 8.0$ Hz)] to C-2 (126.5) and C-6 (122.0), H-5 [7.11(1H, t, $J = 8.0$ Hz)] to C-3 (154.0) and C-7 (136.7), H-1 [a4.38(1H, d, $J = 13.5$ Hz), b4.95(1H,d, $J = 13.5$ Hz)] to C-3 (154.0) and C-10 (103.8), H-8 [6.68 (1H, d, $J = 12.5$ Hz)] to C-2 (126.5), C-6 (122.0) and C-10 (103.8) , H-9 [5.85(1H, d, $J = 12.5$ Hz)] to C-7 (136.7) were observed. HMBC correlations about fragment **1-b** were from H-1′ [a4.29(1H, d, $J = 13.5$ Hz, b4.95(1H,d, $J = 13.5$ Hz)] to C-10′ (104.7) and C-3′ (151.9), from H-4′ [6.61(1H, d, $J = 8.5$ Hz)] to C-2′ (127.9), from H-5′ [6.46(1H, d, $J = 8.5$ Hz)] to C-3′ (151.9), C-6′ (131.2) and C-7′ (134.3), from H-8′ [7.09(1H, d, $J = 12.5$ Hz)] to C-10′ (104.7), from H-9′ [5.91(1H, d, $J = 12.5$ Hz)] to C-7′ (134.3) and C-10′ (104.7). HMBC correlations about fragment **1-c** were from H-5″ [7.00 (1H, t, $J = 8.0$ Hz)] to C-2″ (125.0) and C-3″ (155.9), H-6″ [6.63 (1H, d, $J = 8.0$ Hz)] to C-2″ (125.0) and C-4″ (113.6), H-6″ [6.63 (1H, d, $J = 8.0$ Hz)] to C-8″ (28.0), H-8″ [a6.63(1H, d, $J = 8.0$ Hz), b2.60(1H,t, $J = 8.0$ Hz)], H-9″ [a2.35(1H, dt, $J = 16.0$, 7.5 Hz), b2.24(1H, dt, $J = 16.0$, 7.5 Hz)] and H-11″ [3.53(3H, s)] to C-10″ (173.0).

The connection of fragment **1-b** and fragment **1-a** was further confirmed on the basis of HMBC correlations from H-11 [3.95(1H, m)] to C-10 (103.8) and C-10′ (104.7), H-9 [5.85(1H, d, $J = 12.5$ Hz)] to C-10 (103.8), H-12 [0.91(3H, d, $J = 6.0$ Hz)] to C-11 (66.7), H-11′ [3.88 (1H, d, $J = 6.5$ Hz)] to C-10′ (104.7), H-12′ [0.75(1H, d, $J = 6.5$ Hz)] to C-11′ (66.7). HMBC correlations from H-1″ [3.95(2H, s)] to C-6′ (131.2), C-8′ (129.0) and C-7″ (141.1) and from H-5′ [6.46(1H, d, $J = 8.5$ Hz)] and H-8′ [7.09(1H, d, $J = 12.5$ Hz)] to C-1″ (28.4) determined the connection of fragment **1-b** and fragment **1-c**. The NOESY correlations of H-9 [5.85(1H, d, $J = 12.5$ Hz)] with H-12 [0.91(3H, d, $J = 6.0$ Hz)], H-12 [0.91(3H, d, $J = 6.0$ Hz)] with H-1′ [a4.29(1H, d, $J = 13.5$ Hz),b4.95 (1H,d, $J = 13.5$ Hz)], H-1 [a4.38(1H, d, $J = 13.5$ Hz), b4.95(1H,d, $J = 13.5$ Hz)] with H-12′ [0.75(1H, d, $J = 6.5$ Hz)], H-9′ [5.91(1H, d, $J = 12.5$ Hz)] with H-12′ [0.75(1H, d, $J = 6.5$ Hz)], H-8′ [7.09(1H, d, $J = 12.5$ Hz)] with H-1″ [3.95(2H, s)] suggested the relative configuration of compound **1**. The absolute configuration of **1** was determined by comparison of the experimental and simulated circular dichroism spectra. The result showed that the experimental CD spectrum of **1** and the calculated CD spectrum have similar positive cotton effects in the region 225–275 nm (Fig. 4), which suggest that the absolute configuration of **1** was as shown in Fig. 5.

Alternaria B **(2)** was obtained as light yellow powder (MeOH), $[\alpha]_D^{20}$ —48 (*c* 0.125, MeOH). The molecular formulas of **2** was $C_{25}H_{30}O_8$ on the basis of the ^{13}C NMR, ^1H NMR spectroscopic (Table 2) and HRESIMS data $[M + Na]^+$ ion peak at *m/z* 481.1838. The ^{13}C NMR and HMQC of **2** showed eight sp^2 methine carbons (δ_C 112.5, 114.3, 115.4, 122.0, 128.3, 129.2, 131.9, 132.3), six sp^2 quaternary carbons (δ_C 125.6, 127.2, 136.6, 144.3, 152.1, 154.0), three sp^3 methylene carbons (δ_C 36.6, 56.0 70.6), two sp^3 methine carbons (δ_C 68.0, 69.1), two sp^3 quaternary carbons (δ_C 97.2, 99.6), two methyl groups (δ_C 15.1, 20.1), one oxymethyl carbon (δ_C 48.0). The ^1H NMR spectrum of **2** showed signals attributable to two vicinal sp^2 spin networks [δ 6.77 (1H, d, $J = 8.0$ Hz), 6.80 (1H, d, $J = 8.0$ Hz), 7.08(1H, t, $J = 8.0$ Hz)] and [δ 6.63 (1H, d, $J = 8.0$ Hz), 6.75 (1H, d, $J = 8.0$ Hz), 7.07(1H, t, $J = 8.0$ Hz)]. The HMBC experiments (Fig. 6) only showed the connectivity of partial structures. The whole structure was divided into two fragments as fragment **2-a** and fragment **2-b** (Fig. 7). HMBC data clearly showed one of the aromatic moieties of **2** and the connectivity between group and carbons. HMBC correlations from H-4 [6.77(1H, d, $J = 8.0$ Hz)] to C-2 (127.2) and C-6 (122.0), from

Table 1
^{1}H (500 MHz) and ^{13}C (125 MHz) NMR Data of Compound 1 in DMSO-d_6.

position	δ_H	δ_C	position	δ_H	δ_C
1	a4.38(1H, d, J = 13.5 Hz)b4.95(1H,d, J = 13.5 Hz)	56.6	1′	a4.29(1H, d, J = 13.5 Hz) b4.95(1H,d, J = 13.5 Hz)	57.0
2		126.5	2′		127.9
3		154.0	3′		151.9
3-OH	9.51(1H, s)		3′-OH	9.35(1H, s)	
4	6.79(1H, d, J = 8.0 Hz)	115.0	4′	6.61(1H, d, J = 8.5 Hz)	114.7
5	7.11(1H, t, J = 8.0 Hz)	128.5	5′	6.46(1H, d, J = 8.5 Hz)	127.1
6	6.85 (1H, d, J = 8.0 Hz)	122.0	6′		131.2
7		136.7	7′		134.3
8	6.68(1H, d, J = 12.5 Hz)	131.2	8′	7.09(1H, d, J = 12.5 Hz)	129.0
9	5.85(1H, d, J = 12.5 Hz)	131.1	9′	5.91(1H, d, J = 12.5 Hz)	131.2
10		103.8	10′		104.7
11	3.95(1H, m)	66.7	11′	3.88(1H, d, J = 6.5 Hz)	66.5
12	0.91(3H, d, J = 6.0 Hz)	16.4	12′	0.75(1H, d, J = 6.5 Hz)	15.9
			1′’	3.95(2H, s)	28.4
			2′’		125.0
			3′’		155.9
			3′’–OH	9.33(1H, s)	
			4′’	6.74 (1H, d, J = 8.0 Hz)	113.6
			5′’	7.00 (1H, t, J = 8.0 Hz)	127.5
			6′’	6.63 (1H, d, J = 8.0 Hz)	120.2
			7′’		141.1
			8′’	a6.63(1H, d, J = 8.0 Hz) b2.60(1H,t, J = 8.0 Hz)	28.0
			9′’	a2.35(1H, dt, J = 16.0, 7.5 Hz) b2.24(1H, dt, J = 16.0, 7.5 Hz)	34.7
			10′’		173.0
			11′’	3.53(3H, s)	51.9

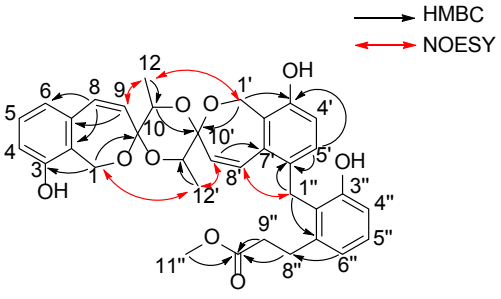

Fig. 2. HMBC correlations of compound **1**.

H-5 [7.08(1H, d, J = 8.0 Hz)] to C-3 (154.0) and C-7 (136.6), from H-1 [4.79(1H, d, J = 13.5 Hz), 3.97 (1H, d, J = 13.5 Hz)] to C-7 (136.6) and C-10 (99.6), from H-8 [6.56(1H, d, J = 12.5 Hz)] to C-2 (127.2) and C-10 (99.6) , from H-9 [5.65(1H, d, J = 12.5 Hz)] to C-7 (136.6) and C-10 (99.6) , from H-12 [0.74(3H, d, J = 6.5 Hz)] to C-10 (99.6) and C-11 (68.0) confirmed the structure of fragment **2-a**. HMBC experiments showed the part of the correlation of fragment **2-b**. We combined part of the HMBC data from H-9′ [1.94(2H, t, J = 5.5 Hz)] to C-7′ (144.3), C-8′ (81.7) and C-10′ (69.1), from H-12′ [3.15(3H, s)] to C-11′ (97.2), from H-13′ [1.15(1H, s)] to C-10′ (69.1) and C-11′ (97.2) and the data described in this document[4] and finally determined the structure of fragment **2-b**. There were two connectable points on the fragment **2-a**, C-10 and C-11. According to the chemical shift law, we further deduced that the fragment **2-b** was connected to the C-10 through an oxygen bridge.

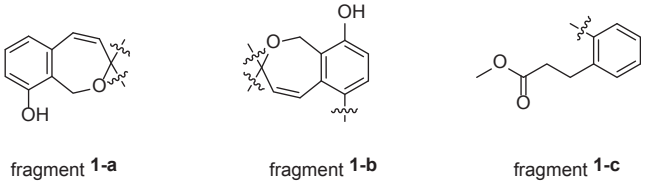

Fig. 3. Structures of fragment **1-a**, fragment **1-b** and fragment **1-c**.

Alternaria C (**3**) was obtained as light yellow powder (MeOH). The molecular formulas of **3** was $C_{11}H_{14}O_4$ on the basis of the ^{13}C NMR, ^{1}H NMR spectroscopic (Table 3) and HRESIMS data $[M+Na]^+$ ion peak at m/z 233.0791. The ^{13}C NMR and HMQC of **3** showed four sp^2 quaternary carbons (δ_C 122.6, 142.9, 156.4, 174.5), three sp^2 methine carbons (δ_C 113.6, 120.1, 129.2), three sp^3 methylene carbons (δ_C 27.9, 35.9, 64.9), one oxymethyl carbon (δ_C 57.7). The ^{1}H NMR spectrum of **3** showed signals attributable to a vicinal sp^2 spin network [δ 6.65 (1H, d, J = 8.0 Hz), 6.68 (1H, t, J = 8.0 Hz), 7.04(1H, d, J = 8.0 Hz)]. The HMBC experiments (Fig. 8) of **3** showed **3** possessed a phenolic OH related with C-3 156.4. The HMBC correlations date from H-4 [6.68(1H, d, J = 8.0 Hz)] and H-6 [6.65(1H, d, J = 8.0 Hz)] to C-2 (122.6) and from H-5 [7.04(1H, t, J = 8.0 Hz)] to C-7 (142.9) and C-3 (156.4) further confirmed the aromatic moiety of **3**. The determination of the structures ultimately depended on the HMBC data apart from the aromatic moiety on the basis of the HMBC correlations from H-1 [4.43(2H, s)] to C-7 (142.9), C-2 (122.6), C-3 (156.4) and C-11 (57.7), from H-11 [3.17(3H, s)] to C-1 (64.9), from H-8 [2.84(2H, t, J = 8.0 Hz)] to C-7 (142.9), C-6 (120.1) and C-10 (174.5), from H-9 [2.57(1H, t, J = 8.0 Hz)] to C-7 (142.9) and C-10 (174.5).

Alternaria D (**4**) was obtained as brown powder (MeOH), $[\alpha]_D^{20}$ —21 (c 0.94, MeOH), which molecular formula was $C_{11}H_{12}O_4$ on the basis of the ^{13}C NMR and ^{1}H NMR spectroscopic data (Table 4) and was confirmed by the HRESIMS data [M + Na] + ion peak at m/z 231.0644. The ^{13}C NMR and HMQC of 4 showed four sp^2 quaternary carbons (δ_C 125.3, 143.1, 152.1, 171.2), three sp^2 methine carbons (δ_C 112.1, 114.7, 129.5), two sp^3 methylene carbons (δ_C 41.4, 70.0), one sp^3 methine carbon (δ_C 80.7), one oxymethyl carbon (δ_C 51.9). The ^{1}H NMR spectrum showed signals attributable to a vicinal sp^2 spin network [δ 6.69 (1H, d, J = 8.0 Hz), 6.71 (1H, t, J = 8.0 Hz), 7.10 (1H, d, J = 8.0 Hz)]. The HMBC experiments (Fig. 9) showed the aromatic moiety of **4** and the connectivity between group and carbons. HMBC correlations about aromatic moiety from H-4 [6.69(1H, d, J = 8.0 Hz)] and H-6 [6.71(1H, d, J = 8.0 Hz)] to C-2 (125.3), H-5 [7.10(1H, t, J = 8.0 Hz)] to C-3 (152.1) and C-7 (143.1) were observed. The OH group signal was confirmed to be a phenolic OH located at C-3 (152.1). The remaining HMBC signals showed the connectivity of partial structures from H-1 [a4.95(1H, d, J = 12.5 Hz), b4.86(1H, d, J = 12.5 Hz)] to C-2 (125.3) and C-7 (143.1) and C-8 (80.7), from H-9 [a2.90(1H, dd, J = 15.5,3.5 Hz), b2.55(1H, dd, J = 15.5,3.5 Hz)] to C-7 (143.1), C-8 (80.7) and C-10 (171.2), from H-11 [3.63(3H, s)] to C-10 (171.2). The above ^{1}H, ^{13}C NMR and HMBC data suggested compound [4] possesses a aromatic ring and a furan ring.

Alternaria E (**5**) was obtained as light yellow amorphous powder (MeOH). The molecular formula of compound **5** was $C_{12}H_{12}O_3$, which was determined by ^{13}C NMR and ^{1}H NMR spectroscopic data (Table 5) and was confirmed by the HRESIMS data [M + Na]$^+$ ion peak at m/z 227.0684. The ^{13}C NMR and HMQC of **5** showed five sp^2 quaternary carbons (δ_C 122.4, 142.9, 153.2 155.3 and 195.5), four sp^2 methine carbons (δ_C 108.2, 114.6, 119.3 and 129.8), two sp^3 methylene carbons

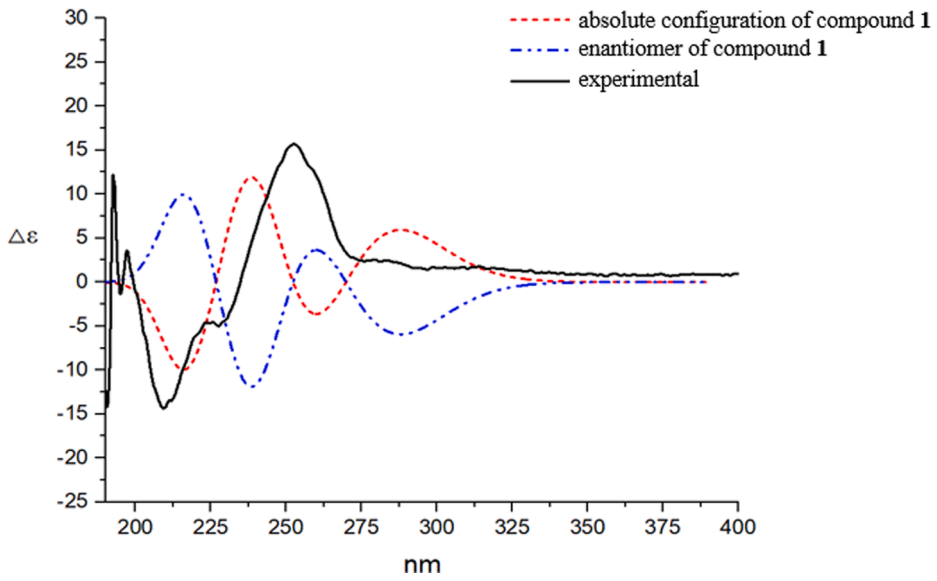

Fig. 4. CD resculls.

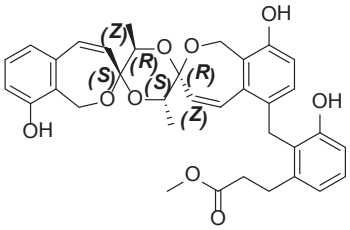

Fig. 5. Absolute configuration of **1**.

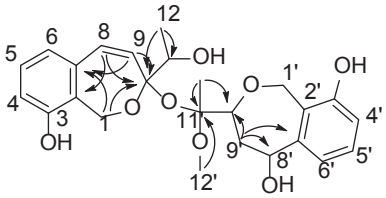

Fig. 6. HMBC correlations of compound **2**.

Table 2
^{1}H (500 MHz) and ^{13}C (125 MHz) NMR Data of Compound 2 in DMSO-d_6.

position	δ_H	δ_C	position	δ_H	δ_C
1	4.79(1H, d, J = 13.5 Hz)3.97(1H, d, J = 13.5 Hz)	56.0	1′	4.85(1H, d, J = 12.0 Hz) 4.99(1H, d, J = 12.0 Hz)	70.6
2		127.2	2′		125.6
3		154.0	3′		152.1
3-OH	9.6(1H, s)		3′-OH	9.6(1H, s)	
4	6.77(1H, d, J = 8.0 Hz)	115.2	4′	6.57(1H, d, J = 8.0 Hz)	112.5
5	7.08(1H, d, J = 8.0 Hz)	129.2	5′	7.07(1H, t, J = 8.0 Hz)	128.3
6	6.80(1H, d, J = 8.0 Hz)	122.0	6′	6.63(1H, d, J = 8.0 Hz)	114.3
7		136.6	7′		144.3
8	6.56(1H, d, J = 12.5 Hz)	132.3	8′	5.26(1H, brs)	81.7
9	5.65(1H, d, J = 12.5 Hz)	131.9	8′-OH	9.6(1H, s)	
10		99.6	9′	1.94(2H, t, J = 5.5 Hz)	36.6
11	3.78(1H, q, J = 6.5 Hz)	68.0	10′	3.98(1H, m)	69.1
11-OH	9.6(1H, s)		11′		97.2
12	0.74(3H, d, J = 6.5 Hz)	15.1	12′	3.15(3H, s)	48.0
			13′	1.15(1H, s)	20.1

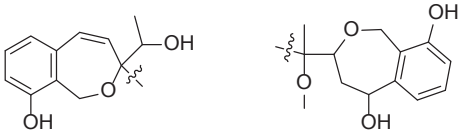

Fig. 7. Structures of fragment **2-a** and fragment **2-b**.

Table 3
^{1}H (500 MHz) and ^{13}C (125 MHz) NMR Data of Compound 3 in DMSO-d_6.

position	δ_H	δ_C
1	4.43(2H, s)	64.9
2		122.6
3		156.4
3-OH	9.42(1H, brs)	
4	6.68(1H, d, J = 8.0 Hz)	113.6
5	7.04(1H, t, J = 8.0 Hz)	129.2
6	6.65(1H, d, J = 8.0 Hz)	120.1
7		142.9
8	2.84(2H, t, J = 8.0 Hz)	27.9
9	2.57(1H, t, J = 8.0 Hz)	35.9
10		174.5
10-OH	12.1(1H, brs)	
11	3.17(3H, s)	57.7

(δ_C 30.6, 63.2), one methyl group (δ_C 26.2). The ^{1}H NMR spectrum showed signals attributable to a vicinal sp^2 spin network [δ 6.78 (1H, d, J = 8.0 Hz), 7.07 (1H, t, J = 8.0 Hz), 6.60 (1H, d, J = 8.0 Hz)]. The HMBC experiments (Fig. 10) showed the connectivity of partial structures. The aromatic moiety of **5** was further confirmed on the basis of HMBC correlations from H-4 [6.78 (1H, d, J = 8.0 Hz)] and H-6 [6.61 (1H, d, J = 8.0 Hz)] to C-2 (122.4) and from H-5 [7.07 (1H, t, J = 8.0 Hz)] to C-3 (155.3) and C-7 (142.9). HMBC correlations from H-1 [5.27

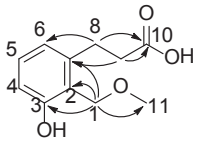

Fig. 8. HMBC correlations of compound **3**.

Table 4
^{1}H (500 MHz) and ^{13}C (125 MHz) NMR Data of Compound 4 in DMSO-d_6.

position	δ_H	δ_C
1	a 4.95(1H, d, J = 12.5 Hz)b 4.86(1H, d, J = 12.5 Hz)	70.7
2		125.3
3		152.1
3-OH	9.79 (1H, brs)	
4	6.69(1H, d, J = 8.0 Hz)	114.7
5	7.10(1H, t, J = 8.0 Hz)	129.5
6	6.71(1H, d, J = 8.0 Hz)	112.1
7		143.1
8	5.46(1H, brd, J = 8.5 Hz)	80.7
9	a2.90(1H, dd, J = 15.5,3.5 Hz)	41.4
	b2.55(1H, dd, J = 15.5,3.5 Hz)	
10		171.2
11	3.63(3H, s)	51.9

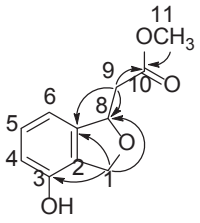

Fig. 9. HMBC correlations of compound **4**.

Table 5
^{1}H (500 MHz) and ^{13}C (125 MHz) NMR Data of Compound 5 in DMSO-d_6.

position	δ_H	δ_C
1	5.27 (2H, s)	63.2
2		122.4
3		155.3
3-OH	9.74 (1H, s)	
4	6.78 (1H, d, J = 8.0 Hz)	114.6
5	7.07 (1H, t, J = 8.0 Hz)	129.8
6	6.61 (1H, d, J = 8.0 Hz)	119.3
7		142.9
8	3.63 (2H, d, J = 5.0 Hz)	30.6
9	5.85 (1H, t, J = 10.0 Hz)	108.2
10		153.2
11		195.5
12	2.16 (3H, s)	26.2

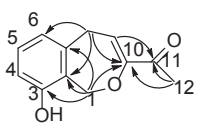

Fig. 10. HMBC correlations of compound **5**.

(2H,s)] to C-3 (155.3), C-7 (142.9) and C-10 (153.2), from H-8 [3.63 (2H, d, J = 5.0 Hz)] to C-2 (122.4), C-10 (153.2) and C-11 (195.5), from H-9 [5.85 (1H, t, J = 10.0 Hz)] to C-7 (142.9), C-10 (153.2) and C-11 (195.5), and from H-12 [2.16 (3H, s)] to C-10 (153.2) and C-11 (195.5)

Table 6
^{1}H (500 MHz) and ^{13}C (125 MHz) NMR Data of Compound 6 in DMSO-d_6.

position	δ_H	δ_C
1	4.42(2H, s)	64.9
2		122.6
3		156.6
3-OH	9.46(1H, brs)	
4	6.69(1H, d, J = 8.0 Hz)	113.7
5	7.03(1H, t, J = 8.0 Hz)	129.3
6	6.64(1H, d, J = 8.0 Hz)	120.1
7		142.6
8	2.85(2H, t, J = 8.0 Hz)	27.8
9	2.57(1H, t, J = 8.0 Hz)	35.5
10		173.3
11	3.59(3H, s)	51.8
11	3.23(3H, s)	57.7

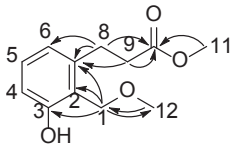

Fig. 11. HMBC correlations of compound **6**.

were also observed. The OH group signal was hence thought to be connected with C-3 (155.3) as the form of a phenolic OH.

Alternaria F (**6**) was obtained as white powder (MeOH). The molecular formulas of **6** was $C_{12}H_{16}O_4$ on the basis of the ^{13}C NMR, ^{1}H NMR spectroscopic (Table 6) and HRESIMS data $[M + Na]^+$ ion peak at *m/z* 247.0953. The ^{13}C NMR and HMQC of **6** showed four sp^2 quaternary carbons (δ_C 122.6, 142.6, 156.6, 173.3), three sp^2 methine carbons (δ_C 113.7, 120.1, 129.3), three sp^3 methylene carbons (δ_C 27.8, 35.5, 64.9), two oxymethyl carbons (δ_C 51.8, 57.7). The ^{1}H NMR spectrum of **6** showed signals attributable to a vicinal sp^2 spin network [δ 6.64 (1H, d, J = 8.0 Hz), 6.69 (1H, t, J = 8.0 Hz), 7.03(1H, d, J = 8.0 Hz)]. The HMBC experiments (Fig. 11) of **6** showed **6** possessed a phenolic OH related with C-3 156.6. The HMBC correlations date from H-6 [6.64(1H, d, J = 8.0 Hz)] to C-2 (122.6) and C-4 (113.7), from H-5 [7.04(1H, t, J = 8.0 Hz)] to C-7 (142.9) and C-3 (156.4) further confirmed the aromatic moiety of **6**. The determination of the structures ultimately depended on the HMBC data apart from the aromatic moiety on the basis of the HMBC correlations from H-1 [4.42 (2H, s)] to C-7 (142.6), C-2 (122.6), C-3 (156.6) and C-12 (57.7), from H-8 [2.85(2H, t, J = 8.0 Hz)] to C-7 (142.6), C-6 (120.1) and C-10 (173.3), from H-9 [2.57(1H, t, J = 8.0 Hz)] to C-7 (142.6) and C-10 (173.3), from H-11 [3.59 (3H, s)] to C-10 (173.3).

Compounds **7**–**13** were known as Pestalospirane A (**7**) [5], Pestalospirane B (**8**)[5], a benzo[*c*]oxepins (**9**)[6], Benzophomopsin A (**10**)[7], Xylarinol A (**12**)[8], Heptacyclosordariolone (**13**) [9].

2.2. Inhibitory effect on SARS-CoV-2 pseudovirus

We used Huh7 cells as host cells, explored the inhibitory effect of compounds **1**–**11** and **13** (the amount of **12** was not enough to be tested) on SARS-CoV-2 pseudovirus and their toxicity to the host cells. At the same time, we used *Chloroquine Phosphate* as a positive control. SI index was used to judge the inhibitory effect: SI greater than 3 was effective (SI = CC_{50}/average EC_{50}). The results (Fig. 12) showed that compounds **1**, **3**, **6**, **8** and **9** had inhibitory effect on the virus, but their SI indexes were different (Fig. 13). Compound **3** (SI = 3.0), compound **6** (SI = 3.7) and compound **1** (SI = 5.9) showed good antiviral effect, compound **8** (SI = 12.7) and compound **9** (SI = 15.2) showed significant antiviral effect. They all had potential druggability.

On the basis of the connection between the structures and inhibition results, we speculated that non-polar substitution of the C-1 was

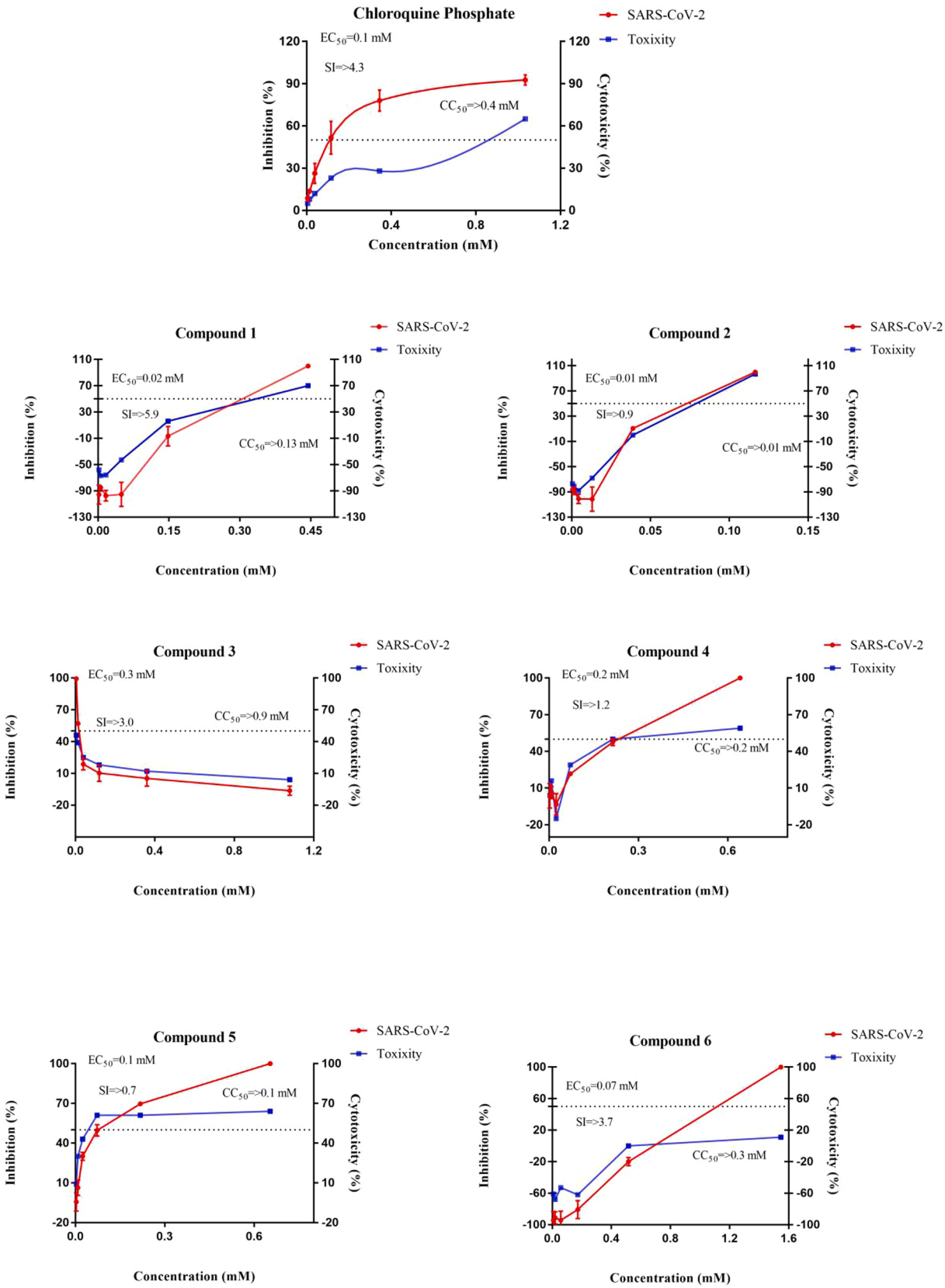

Fig. 12. Inhibition results.

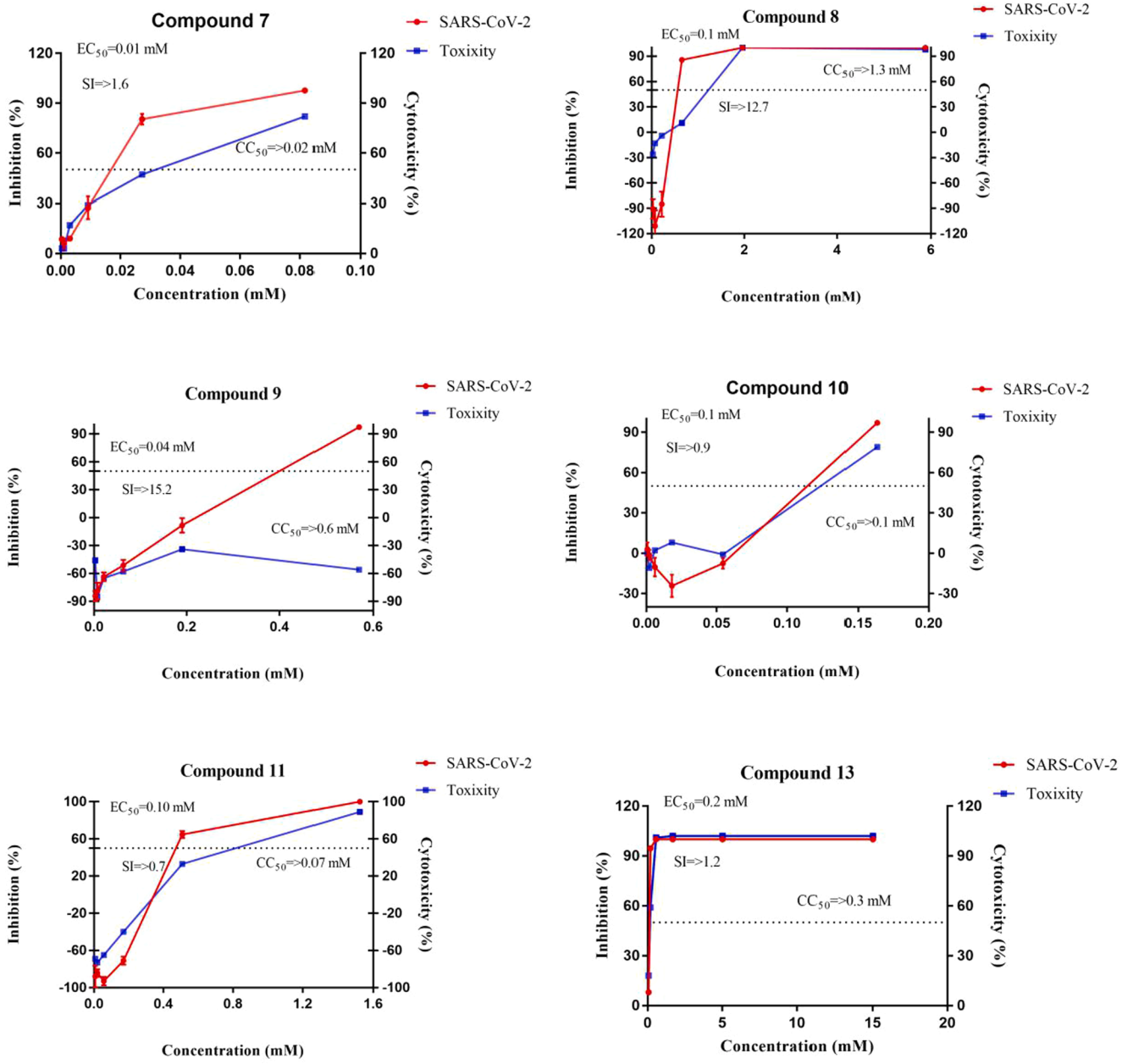

Fig. 12. (*continued*).

beneficial to improve the SI index; formation of a seven-membered ring or ring-opened product was beneficial to improve the SI index; non-polar substitution of side chains of heptacyclic product was beneficial to improve the SI index. For the dimers, they showed higher SI index when their aromatic hydroxyl groups on the same side but it was accompanied by adverse impacts on cells. It also showed higher SI index when the aromatic hydroxyl groups were on the opposite side but a bulky substituent group connected with one side.

3. Disccusion

3.1. Biosynthetic pathway analysis

The core of compounds **3**, **4**, **6**, **11** and **12** constituted by five C_2 units. The six-membered ring was formed by aldol condensation of C-2 and C-7, then it turned into benzene ring through enolization via AA-MA pathway (acetic acid-malonic acid pathway). Finally compounds **3**, **6** and **11** constituted by methylation at different position, compounds 4 and 12 constituted by cyclization at different positions.

The core of compounds **1**, **2**, **5**, **7**, **8**, **9**, **10** and **13** constituted by six *C*2 units. The synthetic pathway of aromatic ring was same as above. Compound **5** was speculated to be finally formed by the C-9 enolization of the seven-membered oxygen-containing ring and C-1 dehydration. Compound **9** was finally formed by the double bond migration. Compound **10** and **13** were finally formed by epoxidation at different positions. Compound **7** and **8** were finally formed by bimolecular condensation. Compound **1** was finally formed by isoelectric replacement between compound **11** and compound **7**. Compound **2** was finally formed by condensation between hemiketal and the second molecule.

4. Experimental section

4.1. General experimental procedures

Highresolution electrospray ionisation mass spectrometry data were measured using an AB Sciex QTOF 4600 mass spectrometer. Using

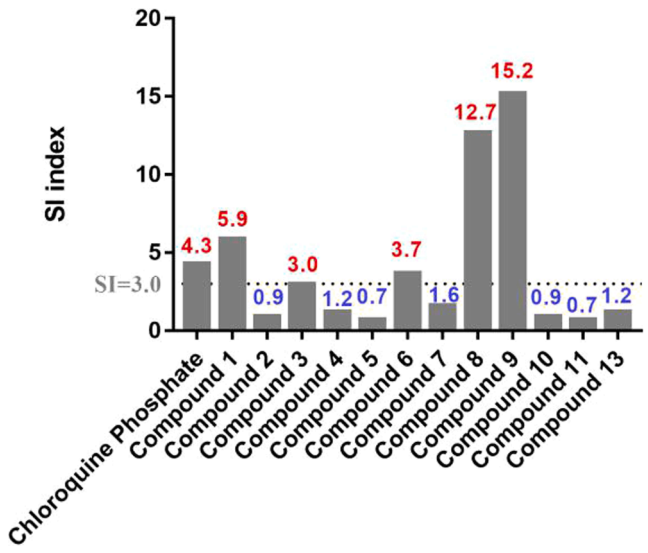

Fig. 13. SI index results.

DMSO-d_6 as solvent, the nuclear magnetic spectrum (^{1}H NMR, ^{13}C NMR, HMBC, HMQC, NOESY, etc.) of the separated compound samples were measured by Bruker AvanceII500 M nuclear magnetic resonance instrument. CD spectra were measured by an J-810-150S spectropolarimeter (JASCO Corporation, Japan). HPLC separation experiments were performed using a system composed of Agilent 1260 (XB C_{18} 10 mm × 250 mm, 5 μm) and Shimadzu LC-20AR (XB C_{18} 10 mm × 250 mm, 5 μm) liquid chromatograph and the UV detection wavelength was 210 nm. For column chromatography (CC), gel LH-20 (Sephadex, Sweden) and silica gel 100–200 mesh and 200–300 mesh (Qingdao Ocean Chemical Co. Ltd, China) were used. Precoated silica gel GF254 (Qingdao Marine Chemistry Co. Ltd, China) plates was used for TLC and PTLC. TLC results were showed at UV wavelengths of 254 nm and 365 nm. The organic reagents used in the general extraction and separation experiments were analytically pure, the organic reagents used in HPLC separation and purification were HPLC grade, and the water is ultrapure water. The sample was concentrated and extracted by a rotary evaporator IKA RV8/HB 10(IKA, Germany). In inhibition rate test, Huh7 cells incubated in CO_2 incubator (SIM, America). Roche Cedex XS Cell counting analyzer (Roche, Sweden) was used in cells counting. The luminescent value of fluorescence detection reagent was read by PerkinElmer EnSight multi-function imaging microplate reader (Promega, America).

4.2. Materials

Plant material was collected from Tibet. The plant endophytic fungu strain used in this experiment was isolated from the leaf part of *Rhodiola tibetica*. It has been identified as Alternaria sp. by molecular biology and morphology and 16sRNA sequencing results. Now it preserved in the School of Life Science and Technology, Dalian University at Dalian City, China. Huh7 cells and SARS-CoV-2 Pseudovirus used in inhibition rate test were from National Institutes for Food and Drug Control, Beijing, China.

4.3. Extraction and isolation of compounds.

The strain HJT-Y7 was inoculated in fungus medium fermentation broth with shaking culture, and then the shaking cultured fermentation broth and mycelium were inoculated into solid medium made by rice and purified water for static fermentation culture 40 days, the culture temperature was 28℃. The solid fermentation product was extracted with methanol. The crude extract (207 g) was obtained by concentrating the fermentation product under low pressure until dryness with a rotary evaporator. A part of crude extract (200 g) was chromatographed on silica gel column eluting with a gradient (100%, 70%, 50%, 30%, 10%, 1 %and 0%, CH_2Cl_2/MeOH) to obtain 12 fractions. Compound **5** (47.7 mg) precipitated from Fr. 3 (1%-0% CH_2Cl_2/MeOH). Fraction 4 (obtained from 1% CH_2Cl_2/MeOH, 6.2 g) was chromatographed on silica gel column eluting with a gradient (90%, 80%, 50%, 30%, 10% and 0%, PE 60–90/EtOAc) to obtain 16 fractions. Compound **4** (2.0 mg) obtained by PTLC ($CHCl_3$/MeOH-9:1) from Fr. 4–2. Fraction 4–2 was chromatographed on gel column and eluted with CH_2Cl_2/MeOH-1:1 to obtain 6 fractions. Fraction 4–2-2 was purified by using preparative HPLC (47% MeOH-H_2O, flow rate 3 mL/min, wavelength 210 nm) to obtain compound **6** (1.2 mg, retention time 23 min). Fraction 4–11 was chromatographed on gel column and eluted with CH_2Cl_2/MeOH-1:1 to obtain 5 fractions. Fraction 4-11-3 was purified by using preparative HPLC (48% MeOH-H_2O, flow rate 3 mL/min, wavelength 210 nm) to obtain compound **3** (26.8 mg, retention time 11 min). Fraction 4–12 was chromatographed on gel column and eluted with CH_2Cl_2/MeOH-1:1 to obtain 5 fractions. Fraction 4–12-4 was purified by using preparative HPLC (70% MeOH-H_2O, flow rate 3 mL/min, wavelength 210 nm) to obtain compound **2** (0.7 mg, retention time 16 min) and compound **1** (1.3 mg, retention time 37 min).

4.3.1. Compound *1*

A light yellow powder; ^{1}H NMR (DMSO-d_6, 500 MHz) and ^{13}C NMR (DMSO-d_6, 125 MHz) in Table 1; HRESIMS *m/z* 623.2248 $[M + Na]^+$ (calcd for $C_{35}H_{36}O_9Na$, 623.2257).

4.3.2. Compound 2

A brown powder; ^{1}H NMR (DMSO-d_6, 500 MHz) and ^{13}C NMR (DMSO-d_6, 125 MHz) in Table 2; HRESIMS *m/z* 481.1838 $[M + Na]^+$ (calcd for $C_{25}H_{30}O_8Na$, 481.1838).

4.3.3. Compound 3

A light yellow powder; ^{1}H NMR (DMSO-d_6, 500 MHz) and ^{13}C NMR (DMSO-d_6, 125 MHz) in Table 3; HRESIMS *m/z* 233.0791 $[M + Na]^+$ (calcd for $C_{11}H_{14}O_4Na$, 233.0790).

4.3.4. Compound 4

A light yellow powder; ^{1}H NMR (DMSO-d_6, 500 MHz) and ^{13}C NMR (DMSO-d_6, 125 MHz) in Table 4; HRESIMS *m/z* 231.0644 $[M + Na]^+$ (calcd for $C_{11}H_{12}O_4Na$, 231.0633).

4.3.5. Compound 5

A light yellow powder; ^{1}H NMR (DMSO-d_6, 500 MHz) and ^{13}C NMR (DMSO-d_6, 125 MHz) in Table 5; HRESIMS *m/z* 227.0684 $[M + Na]^+$ (calcd for $C_{12}H_{12}O_3Na$, 227.0684).

4.3.6. Compound 6

A white powder; ^{1}H NMR (DMSO-d_6, 500 MHz) and ^{13}C NMR (DMSO-d_6, 125 MHz) in Table 6; HRESIMS *m/z* 247.0953 $[M + Na]^+$ (calcd for $C_{12}H_{16}O_4Na$, 247.0946).

4.4. Inhibition rate test

Dissolved the compounds and adjusted the concentration to 10 mg/mL. The initial gradient was a 30-fold dilution, followed by a 3-fold dilution, seven consecutive gradients. Added 100 μl/hole of DMEM complete medium to the virus control (VC), added 150 μl/hole of DMEM complete medium to the cell control (CC), added 142.5 μl/hole to holes B2-B13, and added 100 μl/hole of medium to the remaining holes. Added 7.5 μl of the sample to be tested into holes B2-B13. Gently pipetted the liquid in hole B2-B11 6–8 times, then transferred 50 μl of liquid to the corresponding hole *C*2-C13, and then all holes will be three times diluted. Diluted the SARS-CoV-2 Pseudovirus with DMEM complete medium to 1.3×10^4 TCID50/mL, added 50 μl to each hole in lines

1–13. Put the above 96 hole plate in a cell incubator (37℃, 5% CO_2) and incubated for 1 h. After incubating for 30 min, started digesting Huh7 cells and diluted the cell concentration to 2×10^5 cells/mL. After the incubation, added 100 μl of cells to each hole to make 2×10^4 cells per hole. Put them in a 37℃, 5% CO_2 cell incubator and incubated for 24 h. After incubation, discarded 150 μl of supernatant and added 100 μl Bright-Glo™ Luciferase Detection Reagent, after reacting for 2 min in the dark at room temperature, pipetting repeatedly, transferred 150 μl of liquid to the blank plate. Used PerkinElmer EnSight multi-function imaging microplate reader to read the luminescence value (RLU). The cytotoxicity test process was the same as above, but no pseudovirus was added to each hole to judge the effect of the compounds on cell viability. Calculated the drug EC_{50} and CC_{50} values.

Declaration of Competing Interest

The authors declare that they have no known competing financial interests or personal relationships that could have appeared to influence the work reported in this paper.

Acknowledgements

This work was supported by Excellent Youth Team for Scientific Research, Innovation and Entrepreneurship of Dalian University (XQN202004).

Appendix A. Supplementary material

Supplementary data to this article can be found online at https://doi.org/10.1016/j.bioorg.2021.105309.

References

[1] T. Jin, Analysis of the status quo and path of Tibet's authentic medicinal materials industry, Tibet Agri. Sci. Technol. 42 (02) (2020) 1–3.
[2] R.X. Tan, W.X. Zou, Endophytes: a rich source of functional metabolites, Natural Product Rep. 18 (4) (2001).
[3] J. Newman David, G.M. Cragg, Natural products as sources of new drugs over the last 25 years, J. Nat. Prod. 70 (3) (2007) 461–477.
[4] L. In-Kyoung, et al., Xylarinols A and B, two new 2-benzoxepin derivatives from the fruiting bodies of Xylaria polymorpha, J. Antibiotics 62 (3) (2009) 163–165.
[5] J.R. Kesting, L. Olsen, D. Staerk, M.V. Tejesvi, K.R. Kini, H.S. Prakash, J. W. Jaroszewski, Production of unusual dispiro metabolites in Pestalotiopsis virgatula endophyte cultures: HPLC-SPE-NMR, electronic circular dichroism, and time-dependent density-functional computation study, J. Nat. Prod. 74 (10) (2011) 2206–2215.
[6] Badrinarayanan Sandhya,Squire Christopher J,Sperry Jonathan,Brimble Margaret A. Bioinspired Total Synthesis and Stereochemical Revision of the Fungal Metabolite Pestalospirane B. Organic letters,2017,19(13).
[7] Shiono Yoshihito,Nitto Ayumi,Shimanuki Keiko,Koseki Takuya,Murayama Tetsuya, Miyakawa Tokichi,Yoshida Jun,Kimura Ken-ichi. A new benzoxepin metabolite isolated from endophytic fungus Phomopsis sp. The Journal of antibiotics,2009,62 (9).
[8] Julie Kesting,Dan Staerk,Mysore Tejesvi,Kukkundoor Kini,Harishchandra Prakash, Jerzy Jaroszewski. HPLC-SPE-NMR Identification of a Novel Metabolite Containing the Benzo[c]oxepin Skeleton from the Endophytic Fungus Pestalotiopsis virgatula Culture. Planta Med,2009,75(10).
[9] MARIE LOUISE BOUILLANT, JACQUES BERNILION, JEAN FAVR. New Hexaketides Related to Sordariol in Sordaria macrospora. Zeitschrift für Naturforschung C,1989,44(9-10):719-723. DOI:10.1515/znc-1989-9-100.